The hepatotoxicity of multi-walled carbon nanotubes in mice

2009 Nanotechnology 20 445101

(http://iopscience.iop.org/0957-4484/20/44/445101)

Nanotechnology **20** (2009) 445101 (9pp) doi:10.1088/0957-4484/20/44/445101

The hepatotoxicity of multi-walled carbon nanotubes in mice

Zongfei Ji[1,3], Danying Zhang[1,3], Ling Li[2], Xizhong Shen[1], Xiaoyong Deng[2,4], Ling Dong[1,4], Minhong Wu[2] and Yuanfang Liu[2]

[1] Department of Gastroenterology, Zhongshan Hospital, Shanghai Medical College, Fudan University, Shanghai 200032, People's Republic of China
[2] Institute of Nanochemistry and Nanobiology, Shanghai University, Shanghai 200444, People's Republic of China

E-mail: xydeng@shu.edu.cn and dltalk@tom.com (L Dong)

Received 28 June 2009, in final form 10 September 2009
Published 5 October 2009
Online at stacks.iop.org/Nano/20/445101

Abstract

The hepatotoxicity of two types of multi-walled carbon nanotubes (MWCNTs), acid-oxidized MWCNTs (O-MWCNTs) and Tween-80-dispersed MWCNTs (T-MWCNTs), were investigated with Kunming mice exposed to 10 and 60 mg kg^{-1} by intravenous injection for 15 and 60 d. Compared with the PBS group, the body-weight gain of the mice decreased and the level of total bilirubin and aspartate aminotransferase increased in the MWCNT-exposed group with a significant dose–effect relationship, while tumor necrosis factor alpha level did not show significant statistical change within 60 d. Spotty necrosis, inflammatory cell infiltration in portal region, hepatocyte mitochondria swelling and lysis were observed with a significant dose–effect relationship in the MWCNT groups. Liver damage of the T-MWCNT group was more severe than that of the O-MWCNT group according to the Roenigk classification system. Furthermore, T-MWCNTs induce slight liver oxidative damage in mice at 15 d, which was recovered at 60 d. Part of the gene expressions of mouse liver in the MWCNT groups changed compared to the PBS group, including GPCRs (G protein-coupled receptors), cholesterol biosynthesis, metabolism by cytochrome P450, natural-killer-cell-mediated cytotoxicity, TNF-α, NF-κB signaling pathway, etc. In the P450 pathway, the gene expressions of Gsta2 (down-regulated), Cyp2B19 (up-regulated) and Cyp2C50 (down-regulated) had significant changes in the MWCNT groups. These results show that a high dose of T-MWCNTs can induce hepatic toxicity in mice while O-MWCNTs seem to have less toxicity.

(Some figures in this article are in colour only in the electronic version)

1. Introduction

Due to their unique properties, carbon nanotubes (CNTs) have been demonstrated to be a promising nanomaterial with wide applications, among which their utilization in biomedicine has attracted increasing attention [1]. Recently, many groups have functionalized CNTs with polymers, proteins, nucleic acids and lipids for their biomedical applications. For example, CNTs have been used as substrates for neural growth [2], bone cement [3], biosensors [4], tumor targeting [5, 6] and delivery of drugs, proteins, peptides and nucleic acids, and so forth [1].

While their applications in biomedical and material science continue and broaden, the toxicity issue of CNTs is emerging as one of the most urgent concerns [7]. In the past decade, toxicological studies on CNTs, both *in vitro* and *in vivo*, have been independently reported by various groups. However, these results are not very consistent [8]. Some reports demonstrated that CNTs can induce various inflammatory responses, diffuse interstitial fibrosis and severe pulmonary granuloma formation in mice or rats [9, 10]. Some studies showed that CNTs can induce human fibroblasts [11] and T lymphocyte apoptosis [12] and exhibit cytotoxicity in alveolar macrophages as well [13]. However, some other studies observed no obvious toxicity of properly functionalized or purified CNTs [14]. These conflicting conclusions show that

[3] Z F Ji and D Y Zhang contributed equally to this work.
[4] Authors to whom any correspondence should be addressed.

physical and chemical parameters of CNTs play an important role in the toxicity and biocompatibility of CNTs, including surface functionalization, length, contaminants and so on [14]. In fact, previous studies have revealed that the chemical state of the surface of CNTs may strongly influence tissue response [15]. Chemically treating the surface of CNTs can alter their susceptibility to form agglomerates or to disperse in an environment, as well as to evoke an interaction with the cells responsible for inflammation [16].

Recently, we and many other groups have successfully indicated that CNTs were trapped by the reticuloendothelial system and retained mainly in the liver of mice for a long time after intravenous injection [17–19]. Herein, we selected the liver as the target to investigate the *in vivo* biocompatibility of two types of CNTs differing in their surface chemical state and structure, namely acid-oxidized multi-walled CNTs (O-MWCNTs) and Tween-80-dispersed multi-walled CNTs (T-MWCNTs). The general conditions of mice, pathological changes and gene expressions of liver were monitored, along with the biochemical indexes and TNF-α in blood, the reduced glutathione (GSH) and superoxide dismutase (SOD) activity of liver.

2. Materials and methods

2.1. T-MWCNTs and O-MWCNTs

Pristine MWCNTs (purity > 95%, diameter 10–20 nm, length 5–50 μm, amorphous carbon <3%, ash (catalyst residue) <0.2%) were purchased from Shenzhen Nanotech Port Co., Ltd, China. O-MWCNTs were prepared by the following method. 500 mg pristine MWCNTs were dispersed in a 300 ml 3:1 (v/v) mixture of H_2SO_4 and HNO_3. Following ultrasonication for 4 h at 40 °C, these oxidized MWCNTs were diluted with distilled water and filtered with a cellulose membrane microbore of 0.22 μm. Then the samples were washed with water until the pH of the filtrate is 7. Finally, the black residual products on the membrane were dried in a vacuum drying oven at 60 °C for 24 h. O-MWCNTs were dispersed in PBS before animal experiments.

A subset of the above O-MWCNTs was taken to create T-MWCNTs. The carboxyl groups on O-MWCNTs was detached in an 800 °C oven for 4 h under N_2 atmosphere, and the final products were dispersed in PBS with 1 wt% Tween-80 for animal experiments.

2.2. Animals

All animal experiments were performed in compliance with the institutional ethics committee regulations and guidelines on animal welfare. One hundred healthy male Kunming mice, aged 8 weeks, of clean grade, weighing 25 ± 2 g, were supplied by the experimental animal center of Shanghai Medical College, Fudan University. The mice were housed in cages under a 12 h light–dark cycle with free access to food and drinking water ad libitum. The pelleted diet mainly contained dehulled soybean meal, ground corn, ground wheat, wheat middling, soybean oil, fish meal, ground oats, wheat germ, brewers dried yeast, ground soybean hulls, several types of vitamin, amino acids and other trace metal elements. The drinking water was tap water.

2.3. General experimental design

Kunming mice were divided randomly into five groups ($n = 20$ in each group) including the PBS group (control), O-MWCNT group (10 and 60 mg kg^{-1}) and T-MWCNT group (10 and 60 mg kg^{-1}). After the mice were exposed by intravenous injection, general conditions including appetite, activity and weight were monitored.

Ten mice of each group were sacrificed at 15 and 60 d. The weight of mouse and liver, TNF-α concentration in plasma, reduced GSH and SOD activity in liver homogenate were measured. The following serum biochemistry parameters were also tested: alanine aminotransferase (ALT), aspartate aminotransferase (AST), total bilirubin (TB) and creatinine (Cr). The pathological changes of liver were observed under light and electron microscopes. The gene expression of mice liver was detected by whole genome expression array and real-time PCR analysis.

2.4. Reduced GSH level and SOD activity in liver

The fresh liver was immersed in cold saline and then blotted with filter paper, weighed quickly and homogenized in ice cold preparation buffer (1 mM Tris-HCl + 0.1 mM EDTA-2Na + 0.8% NaCl, pH = 7.4) to yield 10% (w/v) homogenate. Homogenates were centrifuged at 2000 r min^{-1} for 8 min at 4 °C and the supernatants were used immediately for the assays or stored at −80 °C until used for assay. The concentrations of reduced GSH in the supernatants were determined by using spectrophotometric diagnostic kits (Nanjing Jiancheng Biotechnology Institute, China) based on the method of Jollow *et al* [20], using 5,5-dithiobis-2-nitrobenzoic acid for color development. They were calculated by comparison with a standard curve of 0.5 mmol l^{-1} GSH solution. Total SOD levels in the supernatant were also determined by using spectrophotometric diagnostic kits (Nanjing Jiancheng Biotechnology Institute, China) based on the method of Beauchamp and Fridovich [21], which were compared with a standard curve of 10 μg ml^{-1} SOD solution.

2.5. Plasma TNF-α

Plasma TNF-α levels were determined by enzyme-linked immunosorbent assay (ELISA). The commercial kits were bought from BD Biosciences (catalog no. 559732, USA) and carried out according to the manufacturer's directions. The minimum detectable concentration of TNF-α is 5 pg ml^{-1}. The absorbance was measured on a microplate reader at 450 nm and the TNF-α concentration in experimental samples was calculated from a standard curve.

2.6. Histopathological examination

The liver from different groups was fixed in 10% formalin and embedded in paraffin. After routine processing, paraffin sections were cut into 5 μm thickness and stained with

hematoxylin-eosin (H-E). Evaluation was performed under a light microscope (BX51, Olympus Co., Japan).

2.7. Electron microscopy studies

Liver tissue was first sliced into 1 mm × 1 mm × 1 mm and fixed with 2.5% glutaraldehyde in PBS. Then the specimen was post-fixed in 1% osmium tetroxide, dehydrated in a graded alcohol series and embedded in epoxy resin. After peroxide-induced polymerization, the specimen was cut into thin sections with the thickness of approx. 50 nm. These ultrathin liver sections were poststained with uranyl acetate and lead citrate, and inspected with an electron microscope (CM120, Philips Co., The Netherlands).

2.8. Whole genome expression array

The liver of mice in the PBS group and high dose O-MWCNT and T-MWCNT groups were used for gene expression profiling by whole mouse genome microarray technology. There were three samples in each group. The microarray tests were undertaken with the help of KangChen Biotech Company, Shanghai, P R China. The whole mouse genome microarray was obtained from Phalanx Biotech Group. The whole mouse genome microarray contained 29 922 mouse genome probes and 1880 experimental control probes, 31 802 probes in all, and they were highly sensitive 70-mer sense-strand polynucleotide probes. The probe set was an abridged version of the mouse exonic evidence-based oligonucleotide (MEEBO) probe set developed at Stanford University and the University of California, San Francisco. Each probe was spotted onto the array in a highly consistent manner using an innovative non-contact spotting technology adapted and perfected by Phalanx Biotech for microarray manufacturing.

RNA was extracted with Trizol reagent (Invitrogen) according to the kit protocol. After having passed the RNA measurement on the Nanodrop ND-1000 (OD260/280 of all samples between 1.93 and 1.99, OD260/280 $>$ 2) and denaturing gel electrophoresis, double-stranded cDNA template preparation was performed with an Ambion MessageAMP aRNA kit and labeled using the Amersham Mono-functional CyDye.

Fluorescent targets were hybridized to the Mouse Whole Genome OneArrayTM with Phalanx hybridization buffer using cover slides. After overnight hybridization at 50 °C, non-specific binding targets were washed away by three different washing steps and the slides were dried by centrifugation and scanned by a GenePix 4000B microarray scanner (Molecular Devices, Sunnyvale, CA, USA). The Cy3 fluorescent intensities of each spot were analyzed by GenePix Pro 6.0 software (Molecular Devices). The signal intensity of each spot was corrected by subtracting background signals in the immediate surroundings. We filtered out spots that the flags <0 and SNR <3 or control probes. Spots that passed these criteria were normalized by quantile normalization according to the manufacturer's recommendation and tested for differential expression. These differential expressed genes were further analyzed by Agilent GeneSpring GX software (version 10.0).

Table 1. cDNA target genes and primers used for quantitative real-time PCR.

Gene	Forward primer (5′–3′) Reverse primer (5′–3′)	Length of the products (bp)
GAPDH	F: 5′AAGAAGGTGGTGAAGCAGGC3′ R: 5′TCCACCACCCTGTTGCTGTA3′	203
Cyp2B19	F: 5′CACAAAGCCTTCCTCACCGAT3′ R: 5′ACAAGCAAGCAACCCACACTC3′	72
Cyp2C50	F: 5′TTGACCCTGGGCACTTTCTA3′ R: 5′CTTCTCCTGCACATATCCGTTT3′	96
Gsta2	F: 5′AGCCCGTGCTTCACTACTTCA3′ R: 5′GAGGTCATATTTGGTGGCGAT3′	233

2.9. Real-time PCR analysis

Genes in the CYP450 pathway identified from microarray experiment (Gsta2, Cyp2B19 and Cyp2C50) were validated by fluorescence real-time quantitative PCR. The liver of mice in the PBS group and high dose O-MWCNT and T-MWCNT groups were used for further experiments and there were six samples in each group. RNA extraction and cDNAs synthesis processes were repeated as above. The primers were designed using Primer 5.0 software and synthesized by Sangon. GAPDH was used as a reference gene. Primer sequences and source sequence accession numbers are provided in table 1.

A 25 μl real-time PCR reaction system contained 10 μM primer F, 10 μM primer R, 2.5 μl dNTP (2.5 mM each of dATP, dGTP, dCTP and dTTP), 2.5 μl 10× PCR buffer (Promega), 1.5 μl $MgCl_2$ solution (Promega), 1 unit Taq polymerase (Promega), 1 μl cDNA template and added dH_2O to 25 μl. Quantitative real-time PCR was carried out on an Rotor-Gene 3000 Real-time PCR system (Corbett Research) under the following thermal cycle conditions: 3 min at 95 °C, followed by 40 replicates of 20 s at 94 °C, then 20 s at 59 °C, 30 s at 72 °C and extension at 72 °C for 5 min. Electrophoresis on 2% agarose gel and ethidium bromide staining were carried out to observe if PCR products were a single obvious amplified band. All samples were run in duplicate.

After target and housekeeping genes were amplified by PCR, the standard curves were established by the gradient dilution method of the product. The standard curve sample and cDNA sample were added into a real-time PCR reaction system (10 μM primer F, 10 μM primer R, 0.25× Sybergreen (Invitrogen), 2.5 μl dNTP (2.5 mM each), 2.5 μl 10× PCR buffer, 1.5 μl $MgCl_2$ solution, 1 unit Taq polymerase, 1 μl cDNA template and added dH_2O to 25 μl), respectively, and then real-time PCR amplification began under the following thermal cycle conditions: 5 min at 95 °C, followed by 35 replicates of 10 s at 95 °C, then 15 s at 59 °C, 20 s at 72 °C and fluorescence detection at 77–85 °C for 5 s. To establish the dissolution curves, the PCR products were slowly heated from 72 to 99 °C.

According to the DNA standard curve, concentration of each target gene and housekeeping gene in the sample was generated automatically using the Rotor-Gene Real-Time Analysis software 6.0 (build 14). The relative quantification of the target genes was determined by calculating the ratio between the concentration of the target genes and that of

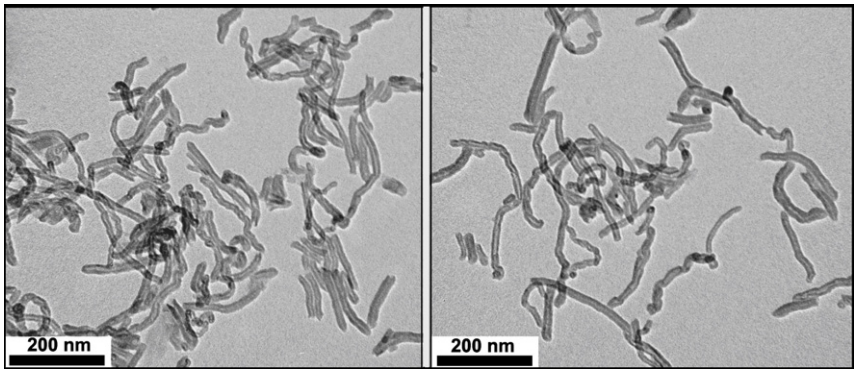

Figure 1. TEM images of O-MWCNTs (left) and T-MWCNTs (right).

the housekeeping gene. In this method, a reference standard was needed to determine the relative quantification of the target gene. The dilution fold of the reference standard was important. For the real-time PCR reaction, the concentration of the target gene is generated by the standard curve. Take the control sample as 1 and the other samples is N-fold of the control.

2.10. Statistical analysis

All the values were represented as mean ±SD. Statistical comparisons between groups were analyzed by SPSS 11.5 statistics software using a one-way ANOVA or Kruskal–Wallis test, and post hoc comparisons were done with an LSD test. P value less than 0.05 was considered significant.

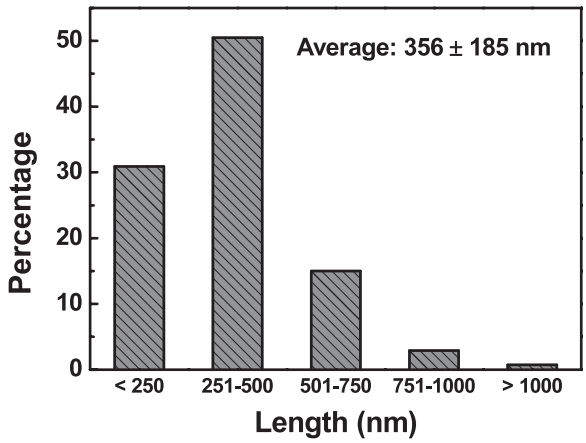

Figure 2. Length distribution of O-MWCNTs.

3. Results

3.1. Characterization of O-MWCNTs and T-MWCNTs

TEM, TGA and ICP-MS were used to characterize the pristine MWCNT samples. As shown in figure 1, no carbon or metal particles were observed in the TEM images of O-MWCNTs and T-MWCNTs. O-MWCNTs and T-MWCNTs were similar in length, mainly ranging from 100 nm to 1 μm with an average of 356 ± 185 nm (based on 580 tubes, figure 2) [22]. TGA and ICP-MS results showed that MWCNT samples contained MWCNTs of relatively high purity (98 wt%) with a small amount of metal impurities of Ni (0.86 wt%), Fe (0.06 wt%) and Co (0.04 wt%) [18].

3.2. General toxicity of O-MWCNTs and T-MWCNTs

MWCNTs had an observable effect on the general behavior of mice; in the MWCNT groups were typically less active than the PBS groups. As shown in figure 3, at a dose of 60 mg kg^{-1}, the body-weight gain of the mice administered with T-MWCNTs was apparently smaller than that of the PBS group for a 60 d period ($P < 0.05$). The liver index significantly decreased in the T-MWCNT group compared with the PBS group for a 15 d period ($P < 0.05$). Figure 4 showed the photos of mouse livers after exposure for 15 or 60 d. The color of livers gradually turns deeper with increasing amount of injected MWNCTs, from blood red in the control group to brown in the 60 mg kg^{-1} MWCNT group, indicating accumulation of MWCNTs in the liver in 60 d.

3.3. Histopathological examination

Figure 5 showed the histological changes of mouse livers in all groups after treatment. No obvious damage was observed in the livers at a dose of 10 mg kg^{-1} for both T-MWCNTs and O-MWCNTs (Roenigk grades 1). In contrary, severe inflammatory cell infiltration in the portal region, cellular necrosis and focal necrosis were seen at a dose of 60 mg kg^{-1} in the T-MWCNT group both at 15 and 60 d (Roenigk grades 2). In the O-MWCNT group, however, only slight inflammatory cell infiltration at 60 d was observed (Roenigk grades 1). These results indicate that T-MWCNTs can cause more severe liver damage than O-MWCNTs.

3.4. Electron microscopy

Electron microscopy was carried out to further investigate the liver damage by T-MWCNTs or O-MWCNTs. The livers of the O-MWCNT group were essentially normal except for slight mitochondria swelling at 15 d but severe swelling at 60 d (figure 6). Severe mitochondrial swelling was observed in the livers of the T-MWCNT group even at 15 d, which was worse at

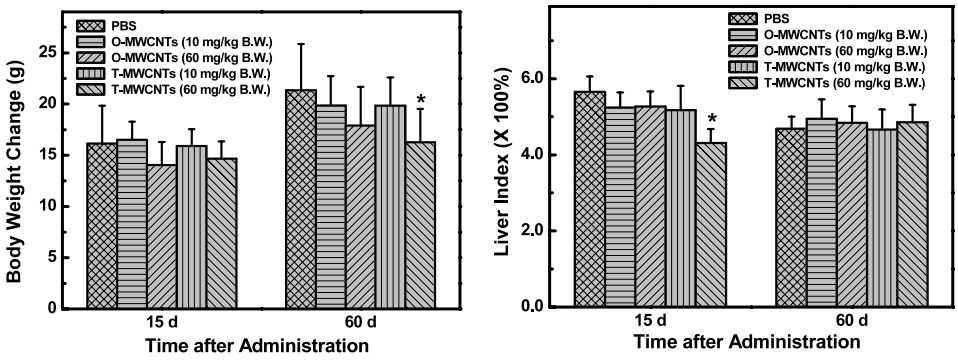

Figure 3. Effects of T-MWCNTs and O-MWCNTs on body-weight gain (left) and liver index (right). Data are presented as mean ± SD, * $P < 0.05$, significantly different from PBS group ($n = 8$–10).

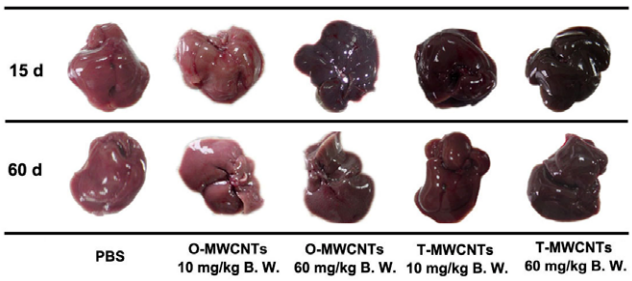

Figure 4. Photos of mouse livers treated with O-MWCNTs or T-MWCNTs.

60 d. In addition, even bile canaliculi expansion, mitochondrial destruction, loss and lysis of mitochondrial crest were observed in the T-MWCNT group at 60 d.

3.5. Oxidative damage in liver

In comparison with the PBS group, significant decrease of reduced GSH level and SOD activity of mice livers in the high dose T-MWCNT group were detected at 15 d (figure 7), while there were no obvious changes among each group at 60 d.

3.6. Biochemical parameters and inflammation index in blood

In comparison with the PBS group, AST for different dosage of T-MWCNT and O-MWCNT groups obviously increased ($P < 0.05$) on the 15th and 60th d. TB also increased 60 d after exposure to T-MWCNTs or O-MWCNTs, while ALT and Cr had no statistical changes (figure 8). There was no statistical difference in TNF-α concentration in the plasma of mice among all the groups at 15 or 60 d (data not shown).

3.7. Whole genome expression array

Out of a total of 29 922 genes, T-MWCNTs exposed mice had 329 genes that were up-regulated and only 31 genes that were down-regulated more than twofold. O-MWCNTs exposed mice were more affected by treatment as 1139 genes were up-regulated and 505 genes were down-regulated over twofold. Among the above changes, we selected several affected pathways with the P-value <0.05 (table 2) which are mainly associated with drug metabolism and liver injury, such as GPCRs (G protein-coupled receptors), cholesterol biosynthesis, metabolism by cytochrome P450 (CYP450), natural-killer-cell-mediated cytotoxicity, TNF-α, NF-κB signaling pathway, etc.

3.8. Real-time PCR analysis

We selected genes in the CYP450 pathway for further real-time PCR analysis to verify the above data (figure 9). The expression of Cyp2B19 and Cyp2C50 was up-regulated and was down-regulated, respectively, in mouse livers in the 60 mg kg^{-1} T-MWCNT and O-MWCNT groups compared with that of the PBS group ($P < 0.01$). However, there were no statistical changes between the two experimental groups. The Gsta2 expression was down-regulated in the 60 mg kg^{-1} T-MWCNT group in comparison with that of both the PBS and the 60 mg kg^{-1} O-MWCNT group ($P < 0.01$), while no significant changes were observed between the PBS and O-MWCNT groups. Data generated from real-time PCR analysis was found to be consistent with the results from the whole genome microarray.

4. Discussion

There are increasing possibilities for humans to contact CNTs because of their extensive applications in the field of biomedical and material science. Therefore, it is essential to thoroughly investigate the toxicity of CNTs [23]. As one of the most important kinds of CNTs in the CNT family, O-MWCNTs are easily obtained and readily dispersed in aqueous solutions and therefore are widely employed as drug carriers to deliver cargoes such as Rhodamine123, DNA and protein into cells, [14]. These drug-functionalized O-MWCNTs will ultimately be administered, metabolized and excreted by animals. Unfortunately there are very few published data on the fate and biological consequences of these drug-functionalized CNTs *in vivo* [19, 24, 25]. Very recently, Yang *et al* demonstrated that the PEG could be cleaved from functionalized CNTs and returned to oxidized CNTs [26]. Thus, the *in vivo* toxicity of covalently functionalized CNTs with defects may, in the long term, come from that of

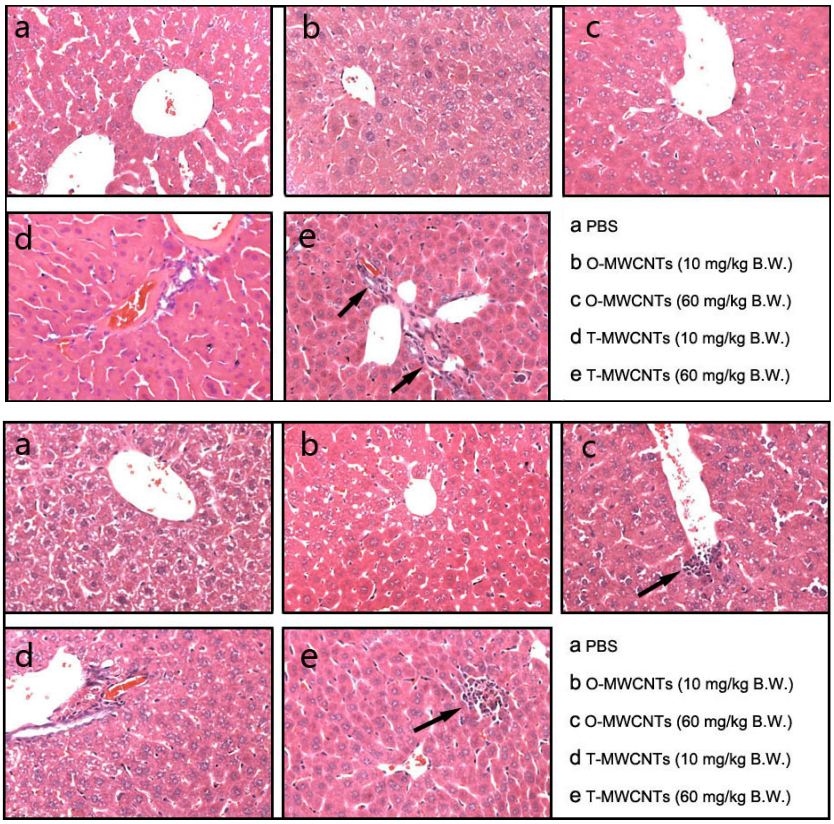

Figure 5. Histological morphology changes of mouse livers exposed to different doses of O-MWCNTs or T-MWCNTs at 15 d (top) and 60 d (bottom) after administration. The black arrows indicate inflammatory infiltrate and low-grade spotty necrosis.

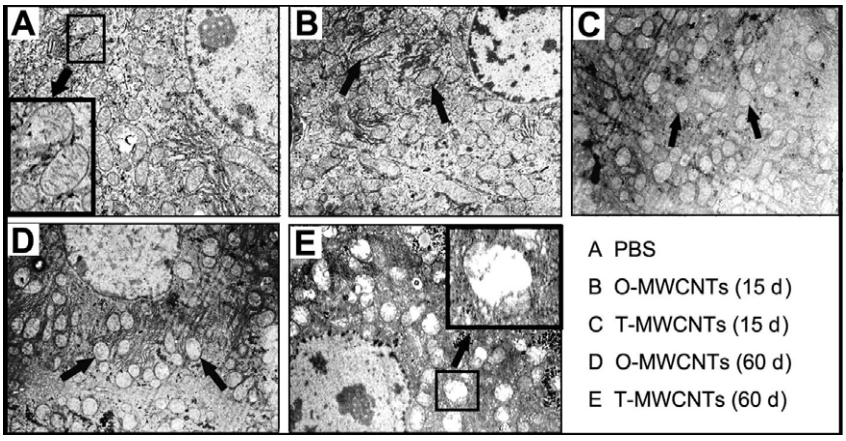

Figure 6. Electron micrographs of mice liver from the T-MWCNT and O-MWCNT groups at a dose of 60 mg kg^{-1}. Mitochondria are indicated by arrows. The inset picture is partial magnification of the small black rectangle and obviously exhibits mitochondrial destruction, loss and lysis of mitochondrial crest.

oxidized CNTs. It is also interesting to investigate the *in vivo* toxicity of non-functionalized MWCNTs. However, non-functionalized MWCNTs are completely insoluble in most solvents and cannot be injected into mice. Fortunately, several papers have shown that surfactant wrapping on CNTs could be easily replaced by biomolecules. For example, Pluronic F108 adsorbed on the nanotube surface could be replaced by serum proteins in rats within 30 min after postintravenous administration [27]. The lipid coating on CNTs could be detached by *Daphnia magna* and ingested as a food source, with the naked CNTs egested in 48 h [28]. Therefore, the Tween-80 adsorbed on the MWCNT surface could be easily detached by biomolecules in mice. The *in vivo* toxicity of T-MWCNTs for a long time, e.g. longer than 15 d, could partly manifest the toxicity of non-functionalized MWCNTs.

In our previous study, mice were exposed by intravenous injection at different dosages (60 and 100 mg kg^{-1}) on 1, 7, 15, 30 and 60 d to evaluate specific toxicity of taurine-

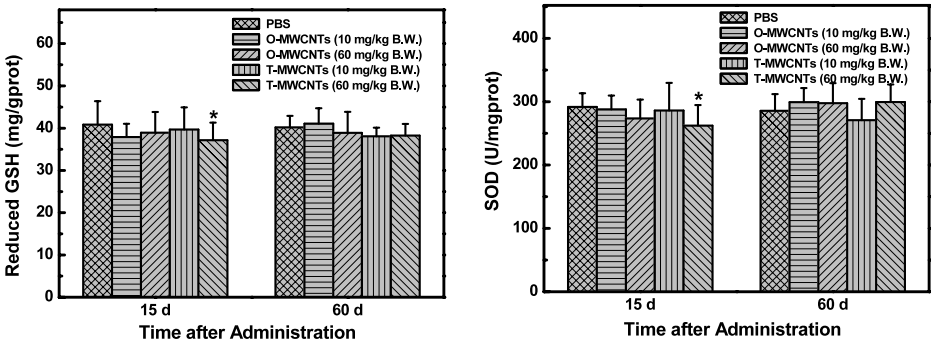

Figure 7. Changes of reduced GSH level and SOD activity in mouse liver exposed to different doses of T-MWCNTs or O-MWCNTs at 15 or 60 d after administration. Data are the mean ± SD of 8–10 mice. * $P < 0.05$ significantly different from the PBS group.

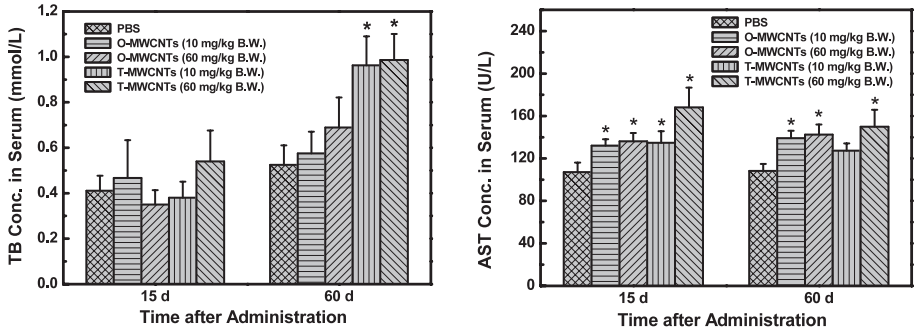

Figure 8. TB and AST concentration in the blood of mice exposed to T-MWCNTs or O-MWCNTs at different doses and different time. Data are presented as mean ± SD, * $P < 0.05$ significantly different from the PBS group ($n = 8$–10).

Table 2. Pathways which are mainly associated with drug metabolism and liver injury by whole genome expression array after exposure of high dose MWCNT groups compared with PBS group ($n = 3$ in all groups, $P < 0.05$, of all the affected genes; there were more genes concentrated in certain pathways, suggesting that the pathways play important roles in the changes of gene expression profile).

Groups compared with PBS group	Pathways	Number of common genes with each pathway	*P*-value
T-MWCNTs	GPCRs	19	0.001 56
	Cholesterol biosynthesis	3	0.001 96
	Natural-killer-cell-mediated cytotoxicity	3	0.026
	Metabolism of xenobiotics by cytochrome P450	3	0.0387
	TNF-α, NF-κB signaling pathway	3	0.0495
O-MWCNTs	GPCRs	17	0.000 985

functionalized MWCNTs [29] and the pilot study showed that these high doses of MWCNTs induced hepatic damage (data not shown in [29]). Therefore, in the current study, we chose two lower doses, 10 mg kg^{-1} (low) and 60 mg kg^{-1} (high), to investigate the *in vivo* toxicology of O-MWCNTs and T-MWCNTs.

The changes of the body weights (figure 3) seemed to show that T-MWCNTs provoked more toxic reaction in mice and the general toxicity of T-MWCNTs had a time–effect relationship and a dose–effect relationship. Figures 5 and 6 showed the inflammation reactions of liver and mitochondrial destructions of hepatocytes in the MWCNT groups. The histological toxic changes were both time-and dosage-dependent; longer time and higher dosage resulted in higher toxicity. Moreover, T-MWCNTs induced more severe histological changes than O-MWCNTs.

Liver injury or metabolism dysfunction are reflected by changes of liver enzymes in serum [30]. The vast majority of ALT in liver exists in the cytoplasm, and only a small amount resides in the mitochondria. The enzymes will penetrate into the blood when the liver cell membrane is damaged. However, the majority of AST exists in the mitochondria in liver cells. When the damage involves hepatocyte mitochondria, the increase of AST will surpass that of ALT. In our study, ALT had no significant changes in every group while the level of AST apparently increased in the T-MWCNT and O-MWCNT groups compared with the PBS group, which was consistent with the damage of hepatocyte mitochondria. Therefore, T-MWCNTs and O-MWCNTs could induce hepatocyte mitochondrial injury to some extent. The changes of TB levels in O-MWCNT or T-MWCNT groups at 60 d, especially in the high dose

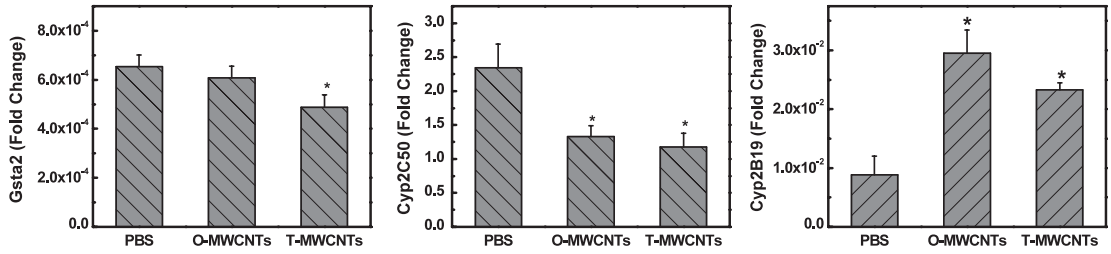

Figure 9. Real-time PCR measurements of genes in CYP450 pathway of different groups ($n = 6$ in all groups, * $P < 0.05$, significantly different from PBS group).

group, became significantly higher than the control group, also suggesting possible hepatocyte injury leading to dysfunction of uptake, combination and excretion of bilirubin. The increase in the TB and AST levels as well as the histological alteration all suggested that T-MWCNTs caused slight liver inflammation, hepatocyte mitochondrial injury and cholestasis in mice.

GSH and SOD are important antioxidants in living creatures, which can protect organisms by scavenging free radicals. Therefore, GSH level and SOD level are important parameters for the antioxidation function of creatures [31]. However, to date, this oxidative stress model to CNT is currently a matter of debate. Sarkar *et al* reported that SWCNTs induce oxidative stress and dictate the activation of specific signaling pathways in keratinocytes [32]. But most of the other related work showed the metal impurity played an important role in the ROS process [8]. Our results (figure 7) suggested that T-MWCNTs induced slight acute liver oxidative stress in mice at 15 d. However, the damage seemed to be recovered soon for there was no obvious change of reduced GSH level and SOD activity among each group at 60 d. Indeed, the recovery was actually typical of a single injection exposure. The insult initially depleted antioxidants, so the organism activated defense pathways. By day 60 post-injection, the mice had successfully dealt with the toxin (through antioxidants, CYP450s, immune response cells, etc) and oxidative indexes had returned to basal levels. Future research with additional intermediary time points is needed to further clarify the trend.

TNF-α is produced by activated macrophages in response to inflammatory processes [33], and is known to have many biological activities including cellular growth, differentiation and apoptosis and inflammation response. In liver, TNF-α is one of the major cytokines that determine the severity of liver toxicity, which in turn mediates acute-phase response of hepatocytes during inflammatory reactions [34]. It also induces hepatocyte proliferation and liver regeneration [35]. To evaluate the inflammatory reaction induced by MWCNTs, the TNF-α level in plasma was quantified by ELISA. The result showed that the TNF-α levels of the experimental groups had no significant statistical changes compared with the control groups ($P > 0.05$), which indicated that MWCNTs did not induce TNF-α-mediated inflammatory reaction to liver.

CYP450 are the main metabolic enzymes that carry out oxidative, peroxidative and reductive metabolism of many structurally diverse compounds including endogenous steroids, fatty acids, retinoids, bile acids, biogenic amines and leucotrienes [36]. CYP450 enzymes are not only essential for the production of cholesterol, steroids, prostacyclins and thromboxane A_2, but are also necessary for the detoxification of foreign chemicals and the metabolism of drugs. CYP450 enzymes can be inhibited or induced by drugs, including warfarin, antidepressants, antiepileptic drugs, etc, resulting in clinically significant drug–drug interactions, unanticipated adverse reactions, therapeutic failures [37] and substance metabolism change. Gsta2 (glutathione S-transferase, alpha 2) is a kind of important CYP450 enzyme, which is involved in GSH metabolism. Therefore, the change of Gsta2 gene expression in liver may correlate to the change of GSH level and lead to liver damage. Besides, Gsta2, Cyp2B19 and Cyp2C50 can promote the metabolism of xenobiotics and drugs by cytochrome P450. Cyp2B19 and Cyp2C50 can also promote lipid and retinol metabolism. The above gene expression changes may ultimately result in exogenous substance and lipid metabolism alternation and generate influence in liver. The real-time PCR result exhibited that Cyp2B19 and Cyp2C50 gene expression levels had significant statistical changes in the T-MWCNT and O-MWCNT groups in comparison with the PBS group, and the Gsta2 gene expression level of the T-MWCNTs group became significantly lower than that of the O-MWCNT and the PBS group, which demonstrated that T-MWCNTs provoked greater alternation of gene expression than O-MWCNTs in the CYP450 pathway.

5. Conclusion

We have conducted comprehensive research to evaluate the hepatic toxicity of T-MWCNTs and O-MWCNTs *in vivo*. The results indicated that these two types of MWCNTs induce slight hepatotoxicity involving inflammatory response, mitochondria destruction and oxidative damage. Compared with T-MWCNTs, O-MWCNTs provoked less change, suggesting that carboxy modification can reduce the hepatotoxicity effect of MWCNTs in mice. MWCNTs can affect several gene pathway expressions in mice, including GPCRs (G protein-coupled receptors), cholesterol biosynthesis, metabolism by cytochrome P450, natural-killer-cell-mediated cytotoxicity, TNF-α, NF-κB signaling pathway, etc.

Acknowledgments

We wish to extend our thanks to Professor Zesheng An from Shanghai University for their kind help. This research

was financially supported by the Science and Technology Commission of Shanghai municipality (0652nm018, 09XD1401800), the China Minister of Science and Technology 973 project (2006CB705604, 2007CB936000), the China Ministry of Health (2009ZX10004-301), the National Natural Science Foundation (20907028) and the Shanghai Leading Academic Discipline Project (S30109).

References

[1] Lu F S, Gu L R, Meziani M J, Wang X, Luo P G, Veca L M, Cao L and Sun Y P 2009 *Adv. Mater.* **21** 139
[2] Hu H, Ni Y C, Mandal S K, Montana V, Zhao B, Haddon R C and Parpura V 2005 *J. Phys. Chem.* B **109** 4285
[3] Shokuhfar T, Makradi A and Titus E 2008 *J. Nanosci. Nanotechnol.* **8** 4279
[4] Gruner G 2006 *Anal. Bioanal. Chem.* **384** 322
[5] McDevitt M R, Chattopadhyay D, Kappel B J, Jaggi J S, Schiffman S R, Antczak C, Njardarson J T, Brentjens R and Scheinberg D A 2007 *J. Nucl. Med.* **48** 1181
[6] Liu Z, Chen K, Davis C, Sherlock S, Cao Q Z, Chen Z Y and Dai H J 2008 *Cancer Res.* **68** 6652
[7] Stern S T and McNeil S E 2008 *Toxicol. Sci.* **101** 4
[8] Shvedova A A, Kisin E R, Porter D, Schulte P, Kagan V E, Fadeel B and Castranova V 2009 *Pharmacol. Ther.* **121** 192
[9] Chou C C, Hsiao H Y, Hong Q S, Chen C H, Peng Y W, Chen H W and Yang P C 2008 *Nano Lett.* **8** 437
[10] Shvedova A A *et al* 2008 *Am. J. Respir. Cell Mol. Biol.* **38** 579
[11] Tian F, Cui D, Schwarz H, Estrada G G and Kobayashi H 2006 *Toxicol. in Vitro* **20** 1202
[12] Bottini M, Bruckner S, Nika K, Bottini N, Bellucci S, Magrini A, Bergamaschi A and Mustelin T 2006 *Toxicol. Lett.* **160** 121
[13] Jia G, Wang H, Yan L, Wang X, Pei R, Yan T, Zhao Y and Guo X 2005 *Environ. Sci. Technol.* **39** 1378
[14] Liu Z, Tabakman S, Welsher K and Dai H J 2009 *Nano Res.* **2** 85
[15] Sayes C M *et al* 2006 *Toxicol. Lett.* **161** 135
[16] Wick P, Manser P, Limbach L K, Dettlaff-Weglikowska U, Krumeich F, Roth S, Stark W J and Bruinink A 2007 *Toxicol. Lett.* **168** 121
[17] Deng X Y, Yang S T, Nie H Y, Wang H F and Liu Y F 2008 *Nanotechnology* **19** 075101
[18] Deng X Y, Jia G, Wang H F, Sun H F, Wang X, Yang S T, Wang T C and Liu Y F 2007 *Carbon* **45** 1419
[19] Liu Z, Cai W B, He L N, Nakayama N, Chen K, Sun X M, Chen X Y and Dai H J 2007 *Nat. Nanotechnol.* **2** 47
[20] Jollow D J, Mitchell J R, Zampaglione N and Gillette J R 1974 *Pharmacology* **11** 151
[21] Beauchamp C and Fridovich I 1971 *Anal. Biochem.* **44** 276
[22] Deng X Y, Xiong D M, Wang H F, Chen D D, Jiao Z, Zhang H J and Wu M H 2009 *Carbon* **47** 1608
[23] Zhao Y L, Xing G M and Chai Z F 2008 *Nat. Nanotechnol.* **3** 191
[24] Villa C H, McDevitt M R, Escorcia F E, Rey D A, Bergkvist M, Batt C A and Scheinberg D A 2008 *Nano Lett.* **8** 4221
[25] Liu Y and Wang H 2007 *Nat. Nanotechnol.* **2** 20
[26] Yang S T, Wang H F, Meziani M J, Liu Y F, Wang X and Sun Y P 2009 *Biomacromolecules* **10** 2009
[27] Cherukuri P, Gannon C J, Leeuw T K, Schmidt H K, Smalley R E, Curley S A and Weisman R B 2006 *Proc. Natl Acad. Sci. USA* **103** 18882
[28] Roberts A P, Mount A S, Seda B, Souther J, Qiao R, Lin S, Ke P C, Rao A M and Klaine S J 2007 *Environ. Sci. Technol.* **41** 3025
[29] Deng X Y, Wu F, Liu Z, Luo M, Li L, Ni Q S, Jiao Z, Wu M H and Liu Y F 2009 *Carbon* **47** 1421
[30] Murakami S, Okubo K, Tsuji Y, Sakata H, Takahashi T, Kikuchi M and Hirayama R 2004 *World J. Surg.* **28** 671
[31] Llacuna L, Marí M, Lluis J M, García-Ruiz C, Fernández-Checa J C and Morales A 2009 *Am. J. Pathol.* **174** 1776
[32] Sarkar S, Sharma C, Yog R, Periakaruppan A, Jejelowo O, Thomas R, Barrera E V, Rice-Ficht A C, Wilson B L and Ramesh G T 2007 *J. Nanosci. Nanotechnol.* **7** 584
[33] Locksley R M, Killeen N and Lenardo M J 2001 *Cell* **104** 487
[34] Mitsias D I, Tzioufas A G, Veiopoulou C, Zintzaras E, Tassios I K, Kogopoulou O, Moutsopoulos H M and Thyphronitis G 2002 *Chin. Exp. Immunol.* **128** 562
[35] Schwabe R F and Brenner D A 2006 *Am. J. Physiol. Gastrointest. Liver Physiol.* **290** G583
[36] Nelson D R *et al* 1996 *Pharmacogenetics* **6** 1
[37] Lynch T and Price A 2007 *Am. Fam. Physician* **76** 391